Laser driven x-ray phase-contrast microscopy of soft tissue samples

Contact *n.carreira-lopes@imperial.ac.uk*

N. C. Lopes

The John Adams Institute for Accelerator Science
Imperial College London, SW7 2AZ, UK &
GoLP/IPFN, Instituto Superior Técnico, Lisboa, Portugal

J. M. Cole, K. Poder, J. C. Wood, S. Alatabi, J. S. J. Bryant, A. E. Dangor, S. Kneip, S. P. D. Mangles, K. Mecseki, Z. Najmudin

The John Adams Institute for Accelerator Science
Imperial College London, SW7 2AZ, UK

P. Abel, N. Ngo, Q. D. Nguyen, M. Winkler

Faculty of Medicine, Department of Surgery & Cancer, Imperial College London, W6 8RF, UK

M. Sroya

Imperial College Healthcare Tissue Bank, Imperial College London, W6 8RF, UK

S. J. Hawkes, C. J. Hooker, D. R. Symes

Central Laser Facility, STFC Rutherford Appleton Laboratory, Chilton, Didcot, OX11 0QX, UK

Introduction

High-resolution visualization of soft tissues is a daily practice in hospitals. Samples collected from patients can be chemically fixed, mounted in paraffin and sliced so the surface of the slices can be imaged with a microscope. In most tissue-slices the contrast is poor and the visualization of the tissue structure down to the cellular level is made using different stains. These histological techniques are the backbone of diagnostics used to detect small-scale lesions in tissues (e.g. prostate or breast cancer).

Recent imaging trials performed with third generation light sources have produced images of tissue structures with comparable resolution to equivalent histologic images [1]. Cancer tissue lesions were identified in both x-ray and histology images of prostate and breast tissue samples [1]. Soft tissues are almost transparent to x-rays and therefore absorption contrast is poor. The tissue structure can, however, be revealed by using phase-contrast x-ray imaging [1]. The simplest phase-contrast modality consists of allowing a propagation distance between the sample and the x-ray detector. Small-scale transverse refractive index gradients in the sample imprint small angle deflections in the x-ray beam that by propagating for enough distance will result in an interference pattern revealing the sample structure.

In a laser-plasma accelerator [2-3], the electrons being accelerated have an oscillatory radial motion component. This betatron motion [4], produces radiation with a broad synchrotron-like (betatron) spectrum characterized by a critical energy (average photon energy in the x-ray beam). The critical energy increases with the electron beam relativistic gamma factor. The total radiated energy in x-rays also scales strongly with the energy of the electron beam. In recent laser-wakefield acceleration experiments it was possible to use the betatron radiation with about 10^9 x-ray photons per shot to produce single shot images of different targets used to characterize the source [5]. Additionally, the source size of the betatron radiation can be as small as one micron opening the possibility of having lens-less micron resolution images. The small source size also means that the beam can be made spatially coherent with the minimum of propagation length, thus making it suitable for phase-contrast imaging [6]. The combination of small source size, spatial coherence, high single-shot brightness and compact size gives laser-plasma-electron driven betatron radiation the potential to be used in future medical imaging diagnostics.

Here we report on an experiment where a laser-driven betatron x-ray source is used in high-resolution imaging of millimetre thick prostate chemically fixed samples.

Experimental Setup

The experiment was performed using the Astra Gemini laser facility (laser pulses with 10 J, 45 fs, 800 nm). The layout of the experimental setup is shown in Fig. 1. The laser pulse was focused with an *f*/20 mirror resulting in a 25 × 32 μm FWHM spot corresponding to an intensity close to 2×10^{19} Wcm^{-2} and a normalized vector potential close to 3. The plasma acceleration structure was created in a gas cell of variable length with sub millimetre apertures in the beam axis for injection and extraction of the beams. The gas cell was injected with helium before each shot to a pressure in the range 20-200 mbar. For the imaging shots reported here, the cell length and pressure were kept at 10 mm and 60 mbar respectively.

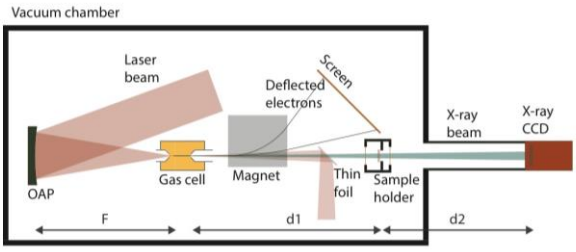

Figure 1: Scheme of the phase-contrast x-ray microscope used for imaging of thick soft-tissue samples

A permanent magnet dipole was placed after the gas cell to deflect the electron beam from the propagation axis (and from the sample holder). The deflected beams were imaged in phosphorescent screens (Kodak-Lanex) to measure the electron energy spectra. The laser beam exiting from the gas cell, co-propagates with the betatron x-ray beam. This transmitted laser energy was reflected off the accelerator axis by a thin aluminium foil that was renewed after each shot. The sample holder consisted of a pressurized box with windows transparent to x-rays. The tissue slices where mounted in the sample holder perpendicular to the x-ray beam. Since a sample image is normally larger than the x-ray detector and much larger than the x-ray beam within the interaction chamber, the sample holder was mounted on a translation stage to make high-resolution scans possible. The x-ray detector was a Andor direct detection CCD camera model iKon M. The distances *d*1 and *d*2 (see Fig. 1) were respectively 0.4 and 3.5 metres (corresponding to a magnification of 8.75, or 2.26 micron of sample per pixel). This microscope was operated at a repetition rate of 0.025 Hz.

X-ray beam

The parameters of the x-ray beam can be estimated using the electron beam parameters [4]. The experimental configuration producing sharpest x-ray images used in this experiment were for electron beams with a single main monoenergetic peak at about 700 MeV containing about 20 pC of charge. An estimate of the number of photons collected in one CCD pixel per keV is presented in Fig. 2 for three different betatron radii: 0.25 μm (green), 0.5 μm (red), and 1.0 μm (blue). For this estimate, we assume that most of the radiation is produced over the two oscillations where the electron beams had maximum energy. This allows us to conclude that: a) the electron beams generated with a 10 J laser (like Astra Gemini) can produce enough intensity for single shot images using the setup presented in Fig. 1; b) the radiation contributing to the imaging will be peaked at 6.5 keV mainly due to the detector quantum efficiency curve; c) the use of lower density plasmas (resulting in lower energy electrons and lower electron beam charge contributing to lower radiation intensity) result in deviation of the peak of the betatron spectra to lower energies close to the maximum quantum efficiency of the detector. This allows for sharper images (by optimizing the source size) whilst improving contrast due to smaller signal to noise ratio because of the reduction in the tail of higher energy photons.

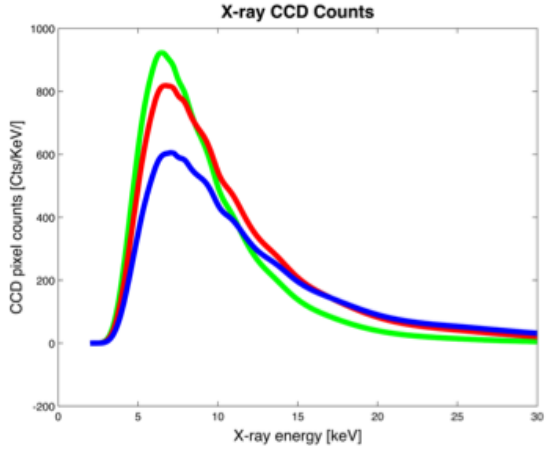

Figure 2: Estimate of the CCD pixel counts for different betatron radii.

The actual measured CCD counts were in good agreement with this estimation (few thousand counts per pixel per shot) providing adequate contrast. The critical energy was measured to be $E_c \approx 30$ keV. This measurement used the comparison of the radiation transmission through a filter pack of different materials [7].

Phase-contrast images of prostate samples

The samples imaged in this experiment were formaldehyde fixed, paraffin embedded prostate slices with thickness between 1 and 3 mm.

A typical single-shot raw image of a fraction of the sample is presented in Fig. 3. This figure was obtained towards the edge of the sample and shows three different absorption zones corresponding to two different thicknesses of the sample and a zone without sample. In this figure, typical phase-contrast features can be easily identified mainly in bubble like structures in the tissue that are common in prostate tissues and can be seen in histologic images when stains are used. In Fig. 4 we present all the images obtained during a scan of a sample.

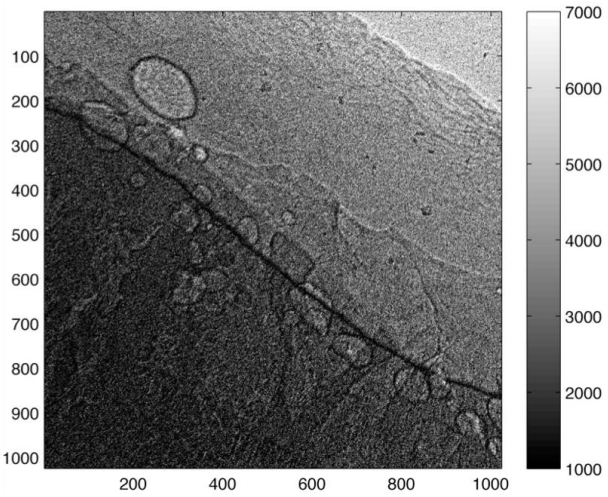

Figure 3: Typical image of a sample fraction.

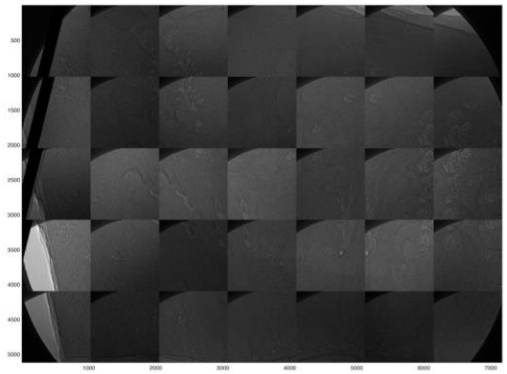

Figure 4: All images obtained during a scan of a sample

The images displayed in Fig. 4 can be used to produce a composite figure of the sample. To produce such a figure the regions with samples on each image are divided by a smoothed version of the same image to compensate for source spatial brightness variations and shot-to-shot brightness variation. The stitching of the images uses a correlation between common features in adjacent images. This step is necessary to compensate the variation of the x-ray beam axis due to the pointing variations of the driving laser beam.

The composite figure resulting from the images shown in Fig. 4 after the process described above is presented in Fig. 5.

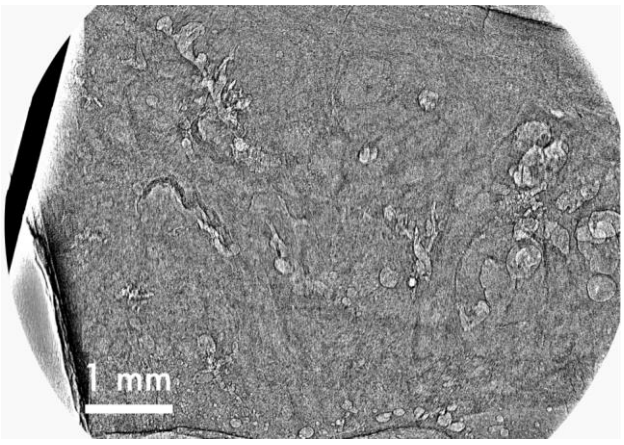

Figure 5: Composite high-resolution image resulting from the combination of the images presented in Fig. 3.

Discussion and conclusion

We were able to produce high-resolution images of three prostate samples similar to the image shown in Fig. 5. The image obtained in Fig. 5 was obtained based on 35 images with some spatial superposition. Each individual image (as shown in Fig. 4) was obtained in a single shot, therefore the image of an 8 mm diameter was obtained in less than one hour. In future, with 1 Hz repetition rate lasers, this can be obtained in less than a minute. The morphology of the soft tissues is clearly visible in the images, making this potentially useful as a medical diagnostic.

The detector, a high-resolution direct detection silicon-based CCD camera, plays an important role in this imaging technique since its quantum efficiency selects the adequate radiation wavelength for samples of this thickness. Thicker samples would require a scintillator-based indirect detection camera. However, imaging of millimetre thick samples may be interesting for medical diagnostic since this is the typical dimension of samples collected by biopsies. In future, with higher repetition rate lasers, a tomography of these samples with similar resolution to the images obtained in this experiment could be obtained in a few minutes. Future work in this research line should include a more detailed study of phase-contrast imaging for different human tissues and the development of the technique for high resolution tomography for samples where a high-resolution imaging can provide additional information for a better medical diagnostic.

Acknowledgements

The authors would like to thank the collaboration of CLF and Imperial College Tissue bank staff that made this experiment possible.

References

1. A. Bravin, P. Coan, P. Suortti, X-ray phase-contrast imaging: from pre- clinical applications towards clinics, Phys. Med. Biol. 58, R1-R35 (2013)

2. T. Tajima and J. M. Dawson, Laser electron accelerator, Phys. Rev. Lett. 43, 267 (1979)

3. S. P. D. Mangles, C. D. Murphy, Z. Najmudin, et al. Monoenergetic beams of relativistic electrons from intense laser–plasma interactions, Nature 431, 535 (2004)

4. E. Esarey, B. A. Shadwick, P. Catravas, and W. P. Leemans, Synchrotron radiation from electron beams in plasma-focusing channels, Phys. Rev. E 65, 056505 (2002)

5. S. Kneip, C. McGuffey, J. L. Martins, et al., Bright spatially coherent synchrotron x-rays from a table- top source, Nat. Phys. 6, 980-983 (2010)

6. S. Kneip, C. McGuffey, F. Dollar, et al., X-ray phase contrast imaging of biological specimens with femtosecond pulses of betatron radiation from a compact laser plasma wakefield accelerator, App. Phys. Lett. 99, 093701 (2011)

7. J. C. Wood, J. M. Cole, A. E. Dangor, et al. High energy, high charge electrons and energetic x-rays from a density tailored gas target, CLF Annual report 2011-2012.